OPTIMAL LINEAR COMBINATIONS SELECTION BASED ON FUZZY CLUSTERING ANALYSIS FOR MULTI-FREQUENCY GNSS

Yuzhao Li [1,2,3], Haowen Yan[1,2,3], Weifang Yang [1,2,3], Shijie Wang [1,2,3], Xiaoning Su [1,2,3]

[1] Faculty of Geomatics, Lanzhou Jiaotong University, 88 Anning West Road, Lanzhou, China - chdlyzhao@163.com, （yanhw，ywfo208，wangshijie，suxiaoning_666）@mail.lzjtu.cn
[2] National-Local Joint Engineering Research Center of Technologies and Applications for National Geographic State Monitoring, 88 Anning West Road, Lanzhou, China - chdlyzhao@163.com, （yanhw，ywfo208，wangshijie，suxiaoning_666）@mail.lzjtu.cn
[3] Gansu Provincial Engineering Laboratory for National Geographic State Monitoring, 88 Anning West Road, Lanzhou, China - chdlyzhao@163.com, （yanhw，ywfo208，wangshijie，suxiaoning_666）@mail.lzjtu.cn

Commission IV, WG IV/5

KEY WORDS: multi-frequency GNSS，fuzzy clustering analysis，optimal linear combination，BDS-3，Geometry-free Multi-frequency Ambiguity Resolution (GF_MCAR)

ABSTRACT:

Currently, satellite navigation and positioning systems, such as BDS, GPS, and Galileo, can broadcast 3 or more navigation signals. In theory, multi-frequency signals can form more high-quality carrier-phase linear combinations, which is conducive to improving the performance of multi-frequency carrier ambiguity resolution (MCAR). In this paper, focusing on the selection of the optimal combinations in the multi-frequency GNSS carrier phase ambiguity resolution, according to the long wavelength of the combinations, the influence of weak ionospheric delay, and low noise, the fuzzy clustering analysis method is used to realize objective selection of multi-frequency optimal linear combinations (e.g., GPS, BDS-2, BDS-3, Galileo) and introduced the total noise level (TNL) for the analysis of the combinations characteristics under different baseline length scenarios. In order to verify the ambiguity resolution performance of the extra-wide lane combinations selected by the fuzzy clustering analysis method, the GF_MCAR model was used to solve the BDS-2, BDS-3 triple-frequency combination ambiguities and the BDS-3 five-frequency combination ambiguities of the baseline JNFG and WUH2. The results manifest that the number of high-quality linear combinations of multi-frequency GNSS increases sharply with the increase of the frequencies number, which is conducive to the formation of combinations with a lower total noise level, and the experiments show that the difference between adjacent epochs of the combination ambiguities of the extra-wide lane obtained by GF_MCAR is basically less than ±0.5 cycles, and the single epoch rounding can be used to directly fix the ambiguity of the extra-wide lane.

1. INTRODUCTION

With the development of our society, people's demands for fast, reliable and high-precision real-time positioning services are increasing. The Global Navigation Satellite System (GNSS) can provide global coverage, continuous, real-time, and all-weather positioning services. It has become a main means to quickly provide location services and has been widely used in real-time disaster monitoring (Zhang et al., 2017; Bai et al., 2019; Zhu et al., 2020), and structure deformation monitoring (Dai et al., 2016; Yi et al., 2018; Xingfu et al., 2018), vehicle navigation (Yang et al., 2016; Cheng et al., 2018), autonomous driving (Wen et al., 2019; Geng et al., 2019) and other fields. The application of multi-GNSS can greatly increase the number of visible satellites, so that fast and high-precision GNSS differential positioning can play an important role in cities where satellite signal interruption frequently occurs or other GNSS difficult areas (Geng et al., 2019). Compared with single-GNSS, multi-GNSS multi-frequency positioning has the following advantages: (1) multi-GNSS can provide more visible satellites, which is beneficial to improve the spatial geometric distribution structures of the satellites and improve positioning accuracy (Yang et al., 2011); (2) multi-frequency GNSS can provide more and better linear combinations, which is beneficial to improve the accuracy and fixed success rate of ambiguity floating-point solution, and improve the reliability of positioning (He et al., 2014; Li et al., 2015); and (3) multi-GNSS can provide more high-altitude satellites, which is conducive to positioning in complex environments such as urban canyons, and can expand the scope of GNSS (Teunissen et al., 2014; Li, 2018).

However, the key to fast and high-precision differential positioning of multi-frequency GNSS is still in the fast and reliable fixation of the integer ambiguity. The multi-frequency carrier ambiguity resolution (MCAR) algorithm is a common method for multi-frequency GNSS ambiguity resolution, which can effectively improve the efficiency and reliability of real-time precision positioning ambiguity resolution in a large-scale or difficult environment. The key lies in how to select the optimal linear combination of observations. Cocard et al. (2008) proposed the number of lanes to characterize the wavelength characteristics of the combinations, and proposed the number of ionospheres to reflect the effect of ionospheric delay. Based on this, Zhang et al. (2015) systematically studied the observation characteristics of the Beidou Regional Satellite Navigation System (BDS-2) triple-frequency carrier phase linear combination; Li et al. (2012 and 2017) used the function extremum method to solve the problem for observation coefficients of the three-frequency optimal combination of BDS and GPS under specific conditions. Some scholars have used the fuzzy clustering algorithm in mathematics to optimize the observation value selection of the GPS triple-frequency optimal combination (Huang et al. 2011) and BDS triple-frequency signal research on the selection of optimal combinations (Li et al., 2020 and 2021).

The above-mentioned research mainly focuses on the selection of GPS, BDS-2 and other triple-frequency carrier phase combinations. At present, China's Beidou Global Satellite Navigation System (BDS-3) can broadcast carrier phase signals at 5 frequency points, Galileo satellites can also broadcast

carrier phase signals at 5 frequency points. In theory, the linear combination of four-frequency and five-frequency can get more combined observations with longer wavelengths, smaller ionospheric delay, and lower noise can further enhance the real-time precision positioning performance (Zhang et al., 2020a, 2020b). However, most of the above-mentioned combination observations are selected by artificial classification. In order to avoid the hard classification of "one or the other" caused by determining the optimal combination based on subjective judgment, this paper uses fuzzy clustering analysis to obtain the optimal combinations of GPS triple-frequency, BDS-2 triple-frequency, BDS-3 triple-frequency, four-frequency and five-frequency, Galileo four-frequency, and the characteristics analysis of the combined observations.

In this study, a preliminary multi-frequency GNSS ambiguity resolution is achieved, using the optimal linear combinations through fuzzy clustering analysis method. First, the theory of multi-frequency GNSS linear combination is given. Then, a fuzzy clustering analysis algorithm is proposed to realize the selection of optimal combinations for multi-frequency GNSS. Finally, in order to verify the performance of the optimal extra-wide lane combinations selected by the fuzzy clustering analysis method, the geometry-free multi-frequency carrier ambiguity resolution (GF_MCAR) method is used to solve the short-baseline BDS-2, BDS-3 triple-frequency combined ambiguity and BDS-3 five-frequency combined ambiguity.

2. GNSS MULTI-FREQUENCY LINEAR COMBINATION

Suppose that the multi-frequency signals broadcast by GNSS are, in descending order of frequency f_1、f_2、…、f_k, and k represents the number of GNSS frequencies (k≥3). According to the GNSS linear combination theory, the multi-frequency GNSS combination frequency, wavelength, double-difference ambiguity can be expressed as:

$$f_{(k)} = i_1 \cdot f_1 + i_2 \cdot f_2 + \cdots + i_k \cdot f_k \tag{1}$$

$$\lambda_{(k)} = \frac{c}{i_1 \cdot f_1 + i_2 \cdot f_2 + \cdots + i_k \cdot f_k} \tag{2}$$

$$N_{(k)} = i_1 \ N_1 + i_2 \ N_2 + \cdots + i_k \ N_k \tag{3}$$

In the formula, i_k is the integer coefficient of the combined observation; c is the speed of light in vacuum.

The corresponding double-difference carrier phase linear combined observation of multi-frequency GNSS can be expressed as:

$$\Phi_{(k)} = \frac{i_1 \cdot f_1 \cdot \varphi_1 + i_2 \cdot f_2 \cdot \varphi_2 + \cdots + i_k \cdot f_k \cdot \varphi_k}{i_1 \cdot f_1 + i_2 \cdot f_2 + \cdots + i_k \cdot f_k} \tag{4}$$

In the formula, $\Phi_{(k)}$ represents the double-difference carrier phase observation after k frequency combinations; φ_k represents the double-difference phase observation of the k-th frequency.

According to the definition of the number of lanes (Cocard et al., 2008), the combined observation frequency of multi-frequency signals can be expressed as:

$$f_{(k)} = i_1 \cdot f_1 + i_2 \cdot f_2 + \cdots + i_k \cdot f_k = \left(i_1 \cdot n_1 + i_2 \cdot n_2 + \cdots + i_k \cdot n_k\right) \cdot f_0 = L_{(k)} \cdot f_0 \tag{5}$$

Assuming that the observation noise of the carrier phase of each frequency is equal and independent, and satisfies $\varepsilon_{\varphi_1} = \varepsilon_{\varphi_2} = \cdots = \varepsilon_{\varphi_k} = \varepsilon_\varphi$, the combined observation noise of the carrier phase in cycles is:

$$\varepsilon_{(k)} = \sqrt{i_1^{\,2} \cdot \varepsilon_{\varphi_1}^2 + i_2^{\,2} \cdot \varepsilon_{\varphi_2}^2 + \cdots + i_k^{\,2} \cdot \varepsilon_{\varphi_k}^2} = \sqrt{i_1^{\,2} + i_2^{\,2} + \cdots + i_k^{\,2}} \cdot \varepsilon_\varphi = T_{(k)} \cdot \varepsilon_\varphi \tag{6}$$

In the formula, $T_{(k)}$ represents the combined observation noise amplification coefficient in cycle, and is only related to the combination coefficient. The greater the sum of squares of the coefficient, the greater the combination noise.

$\beta_{(k)}$、$\theta_{(k)}$, represents the first and second order ionospheric delay scale factors, in the following form:

$$\beta_{(k)} = \frac{f_1^2\left(i_1/f_1 + i_2/f_2 + \cdots + i_k/f_k\right)}{i_1 \cdot f_1 + i_2 \cdot f_2 + \cdots + i_k \cdot f_k} \tag{7}$$

$$\theta_{(k)} = \frac{f_1^3\left(i_1/f_1^2 + i_2/f_2^2 + \cdots + i_k/f_k^2\right)}{i_1 \cdot f_1 + i_2 \cdot f_2 + \cdots + i_k \cdot f_k} \tag{8}$$

Assuming the accuracy of each frequency and phase observation value is equal, then the carrier phase combined observation value accuracy is:

$$\sigma_{\varphi_{(k)}}^2 = \frac{\left(i_1 \cdot f_1\right)^2 \cdot \sigma_{\varphi_1}^2 + \left(i_2 \cdot f_2\right)^2 \cdot \sigma_{\varphi_2}^2 + \cdots + \left(i_k \cdot f_k\right)^2 \cdot \sigma_{\varphi_k}^2}{\left(i_1 \cdot f_1 + i_2 \cdot f_2 + \cdots + i_k \cdot f_k\right)^2} \tag{9}$$

Among them, $\mu_{(k)}$ is defined as the noise factor, and the form is as follows:

$$\mu_{(k)}^2 = \frac{\left(i_1 \cdot f_1\right)^2 + \left(i_2 \cdot f_2\right)^2 + \cdots + \left(i_k \cdot f_k\right)^2}{\left(i_1 \cdot f_1 + i_2 \cdot f_2 + \cdots + i_k \cdot f_k\right)^2} \tag{10}$$

According to the GNSS combination theory, linear combinations should meet the four basic principles of having a longer wavelength, a small ionospheric delay, and a small noise, and maintaining the integer characteristics of ambiguity. Table 1. lists the frequency band and frequencies of the multi-frequency signals of each GNSS system. The combined observations satisfying $i_k \in [-10,10]$, $\lambda_{(k)} \geq 2.93m$, $|\beta_{(k)}| \leq 4$, $T_{(k)} \leq 15$, $\mu_{(k)} \leq 250$ in each GNSS system are regarded as high-quality extra-wide lane combined signals.

Figure 1. shows the numbers statistical results of high-quality extra-wide lane combined signals of GPS and BDS-2 triple-frequency, Galileo four- frequency, and BDS-3 triple-frequency, four- frequency, and five-frequency.

Table 1. Frequency band and frequency of multi-GNSS and multi-frequency (unit: MHz)

System	Freq. Num.	Freq. Band / Frequency (MHz)				
BDS-2	Three	B1	B2	B3		
		1561.098	1207.14	1268.52		
GPS	Three	L1	L2	L5		
		1575.42	1227.6	1176.45		
BDS-3	Three	B1C	B3I	B2a		
		1575.42	1268.52	1176.45		
	Four	B1C	B3I	B2a	B1I	
		1575.42	1268.52	1176.45	1561.098	
	Five	B1C	B3I	B2a	B1I	B2b
		1575.42	1268.52	1176.45	1561.098	1207.14
Galileo	Four	E1	E5a	E5b	E6	
		1575.42	1176.45	1207.14	1278.75	
	Five	E1	E5a	E5b	E6	E5
		1575.42	1176.45	1207.14	1278.75	1191.795

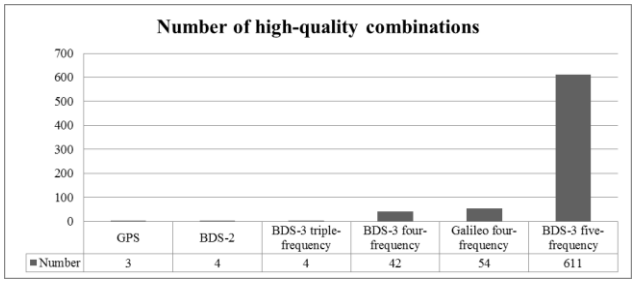

Figure 1. The statistical of multi-GNSS and multi-frequency high-quality extra-wide-lane combinations

It can be seen from Figure 1 that the number of high-quality extra-wide lane combined signals increases sharply with the increase in frequency. Among them, the number of combined signals of five-frequency high-quality extra-wide lanes is about 150 times that of three-frequency, and about 12 times of four-frequency.

According to the multi-frequency carrier ambiguity resolution model, three-frequency, four-frequency and five-frequency MCAR models need to choose 3, 4, and 5 independent linear combinations respectively, and one of the narrow lane combinations must be included. Because the combination of extra-wide lanes is easier to fix the ambiguity, it is preferred to choose 2, 3, 4 optimal extra-wide lane combinations and another narrow lane combination to construct MCAR models at different frequencies. In this paper, fuzzy clustering analysis is used to select the corresponding number of optimal extra-wide lane combinations from the high-quality signal combinations for multi-frequency carrier phase ambiguity resolution.

3. FUZZY CLUSTERING ANALYSIS METHOD

Fuzzy clustering analysis achieves effective data classification through data standardization, calibration (building a fuzzy similarity matrix) and clustering. This article will use this method to select GNSS multi-frequency carrier phase extra-wide lane combinations.

1) Establish the original data matrix

$$\begin{bmatrix} x_{11} & x_{12} & \cdots & x_{1m} \\ x_{21} & x_{22} & \cdots & x_{2m} \\ \vdots & \vdots & \vdots & \vdots \\ x_{t1} & x_{t2} & \cdots & x_{tm} \end{bmatrix} \quad (11)$$

In the matrix, $x_i = (x_{i1}, x_{i2}, x_{i3}, \cdots, x_{it})(i = 1,2,\cdots,t)$ is m indicators of t classification objects are used to represent the characteristics of each classification object. The $L_{(k)}$、$\beta_{(k)}$、$T_{(k)}$ and $\mu_{(k)}$ of the observations of each combination are used as the evaluation index for each combination, and the optimal characteristic value of the evaluation index in the selected combination is used to form a virtual theoretical optimal extra-wide lane combination to jointly construct the original data matrix.

2) Data standardization

The dimension of the original data matrix is not uniform. In order to eliminate the influence of dimension, it needs to undergo translational standard deviation transformation and range transformation to make the transformed value in the interval [0,1].

Translation • Standard Deviation Transformation

$$x'_{ik} = \frac{x_{ik} - \overline{x_k}}{s_k} \quad (i=1,2, \ldots,t; k=1,2, \ldots,m) \quad (12)$$

where

$$\overline{x_k} = \frac{1}{t}\sum_{i=1}^{t} x_{ik}, \quad s_k = \sqrt{\frac{1}{t}\sum_{i=1}^{t}\left(x_{ik} - \overline{x_k}\right)^2} \quad (13)$$

Translation • Range Transformation

$$x''_{ik} = \frac{x'_{ik} - \min\limits_{1\le i\le t}\{x'_{ik}\}}{\max\limits_{1\le i\le t}\{x'_{ik}\} - \min\limits_{1\le i\le t}\{x'_{ik}\}} \quad (k=1,2, \ldots,m) \quad (14)$$

3) Calibration (build fuzzy similarity matrix)

This step aims to establish the fuzzy similarity matrix and the degree $r_{ij} = R(x_i, x_j)$ of similarity between the classified object x_i and x_j. This article uses the number product method to calibrate, that is, to determine the degree of similarity between the classified objects and establish a fuzzy similarity matrix. The specific method is as follows:

$$r_{ij} = \begin{cases} 1, & i = j \\ \dfrac{1}{M}\sum\limits_{k=1}^{m} x_{ik} \bullet x_{jk}, & i \neq j \end{cases} \quad (15)$$

$$M = \max_{i \neq j} \left(\sum_{k=1}^{m} x_{ik} \bullet x_{jk} \right) \quad (16)$$

Obviously $|r_{ij}| \in [0,1]$, if there is a negative value in r_{ij}, it can also be said as $r'_{ij} = \frac{r_{ij}+1}{2}$, then $r'_{ij} \in [0,1]$.

4) Clustering analysis

In order to classify, the fuzzy similarity matrix needs to be transformed into a fuzzy equivalent matrix through the transfer closure method. According to the properties of the fuzzy similarity matrix, the transfer closure of the fuzzy similarity matrix is obtained by the quadratic method, and the resulting transfer closure is fuzzy equivalent matrix, and then complete the fuzzy clustering analysis. According to the close relationship between each combination and the virtual theoretical optimal extra-wide lane combination, the optimal combinations can be determined.

4. MULTI-FREQUENCY LINEAR COMBINATION OF EACH GNSS SYSTEM

In practical applications, in order to better evaluate the characteristics of each combination, the concept of Total Noise Level (TNL) is introduced:

$$\sigma_{\mathrm{TNL}} = \frac{1}{\lambda_{(k)}} \sqrt{\sigma_{orb}^2 + \sigma_{trop}^2 + \beta_{(k)}^2 \cdot \sigma_{I_1}^2 + \theta_{(k)}^2 \cdot \sigma_{I_2}^2 + \sigma_{\varepsilon_{(k)}}^2} = \min \quad (17)$$

In the formula, σ_{TNL} represents the total noise level of the phase observation, in units of cycle; σ_{orb} represents the orbit error; σ_{trop} represents the tropospheric delay error; σ_{I_1} and σ_{I_2} represents the first-order and second-order ionospheric delay errors, respectively, and $\sigma_{\varepsilon_{(k)}}$ represents the carrier phase observation noise.

Assuming three scenarios: I, short and medium baseline (d≤100km), II, medium and long baseline (100 < d ≤200km), III, long baseline (d>200km). The accuracy of each error is shown in Table 2.

Table 2. The specific error precisions of double-differenced phase observations under different baseline lengths （Unit: cm）

	σ_{orb}	σ_{trop}	σ_{I_1}	σ_{I_2}	$\sigma_{\varepsilon_{(k)}}$
I	0.5	1	10	0.5	1
II	1	2.5	40	1	1
III	10	20	100	2	1

The following gives the fuzzy clustering analysis method to select each GNSS multi-frequency optimal extra-wide lane combinations and related parameters, respectively.

Table 3. Optimal combinations and parameters of triple-frequency signals for BDS-2/GPS/BDS-3

System	i_1	i_2	i_3	$\lambda_{(k)}$/m	$\beta_{(k)}$	$\theta_{(k)}$	$\mu_{(k)}$	$L_{(k)}$	$T_{(k)}$	σ_{TNL} /cycle		
										I	II	III
BDS-2	1	-5	4	**6.3707**	**0.6521**	**3.8892**	172.6135	**23**	6.4807	0.0109	0.0416	0.1089
	0	1	-1	4.8842	-1.5915	-4.0167	**28.5287**	30	**1.4142**	0.0330	0.1307	0.3295
GPS	1	-6	5	3.2561	**-0.0744**	**1.4491**	103.8007	9	7.8740	0.0056	0.0135	0.0730
	0	1	-1	**5.8610**	-1.7186	-4.5068	**33.2415**	**5**	**1.4142**	0.0297	0.1176	0.2961
BDS-3	1	-4	3	**9.7684**	2.5487	10.7901	207.8346	**15**	5.0990	0.0267	0.1050	0.2628
	0	1	-1	3.2561	**-1.6631**	**-4.2926**	**18.7909**	45	**1.4142**	0.0517	0.2049	***0.5160***

Table 4. Optimal combinations and parameters of four-frequency signals for BDS-3/Galileo

System	i_1	i_2	i_3	i_4	$\lambda_{(k)}$/m	$\beta_{(k)}$	$\theta_{(k)}$	$\mu_{(k)}$	$L_{(k)}$	$T_{(k)}$	σ_{TNL} /cycle		
											I	II	III
	1	-1	0	0	**20.9323**	**-1.0092**	**-2.0276**	154.8580	**7**	**1.4142**	0.0049	0.0194	0.0494
BDS-3	-3	3	1	-1	6.1053	-2.2353	-6.2745	140.0065	24	4.4721	0.0371	0.1469	0.3685
	-2	2	1	-1	4.7266	-1.9584	-5.3155	**75.0671**	31	3.1623	0.0419	0.1662	0.4176
	0	0	1	-1	**9.7684**	-1.7477	-4.6212	54.9232	**3**	**1.4142**	0.0181	0.0718	0.1806
Galileo	0	1	-2	1	7.3263	**-1.5030**	**-3.6728**	72.6920	4	2.4495	0.0208	0.0823	0.2077
	0	1	-1	0	4.1865	-1.6079	-4.0793	**24.5569**	7	**1.4142**	0.0389	0.1541	0.3883

Table 3 to Table 5 respectively shows the optimal extra-wide lanes combinations and parameters of GNSS three-frequency, four-frequency, and five-frequency selected by the fuzzy clustering analysis method. According to the statistical results, except for the TNL exceeds 0.5 cycles of the BDS-3 triple-frequency extra-wide lane combination (0, 1, -1) under the long baseline condition, the TNL of other extra-wide lane combination is less than 0.5 cycles.

Table 5. Optimal combinations and parameters of BDS-3 five-frequency signals

i_1	i_2	i_3	i_4	i_5	$\lambda_{(k)}$/**m**	$\beta_{(k)}$	$\theta_{(k)}$	$\mu_{(k)}$	$L_{(k)}$	$T_{(k)}$	σ_{TNL} /**cycle**		
											I	II	III
-1	1	0	1	-1	**18.3158**	-2.3939	-6.8907	170.1926	**8**	2.0000	0.0132	0.0524	0.1315
0	0	1	-2	1	9.7684	**-1.4940**	**-3.6353**	96.7798	15	2.4495	0.0155	0.0614	0.1548
0	0	0	1	-1	9.7684	-1.7477	-4.6212	**54.9232**	15	**1.4142**	0.0181	0.0718	0.1806
1	-1	0	1	-1	6.6603	-1.5127	-3.7960	61.8882	22	2.0000	0.0230	0.0911	0.2299

5. EXPERIMENTAL ANALYSIS

In this paper, in order to verify the performance of extra-wide lane combination in fuzzy clustering analysis, the short baseline BDS-2 and BDS-3 measured data of the 2020.294 days MGEX JFNG (receiver: TRIMBLE ALLOY, antenna: TRM59800.00) and WUH2 (receiver: JAVAD TRE_3 antenna: JAVRINGANT_G5T) stations were processed by GF_MCAR method. The data sampling interval is 30s, and the satellite cut-off altitude is 10°. The difference results of adjacent epochs for three-frequency combination ambiguity of BDS-2 C02, C06, C13 and C16 satellites, and three-frequency and five-frequency combination ambiguity for BDS-3 C34 and C40 satellites are given below, respectively.

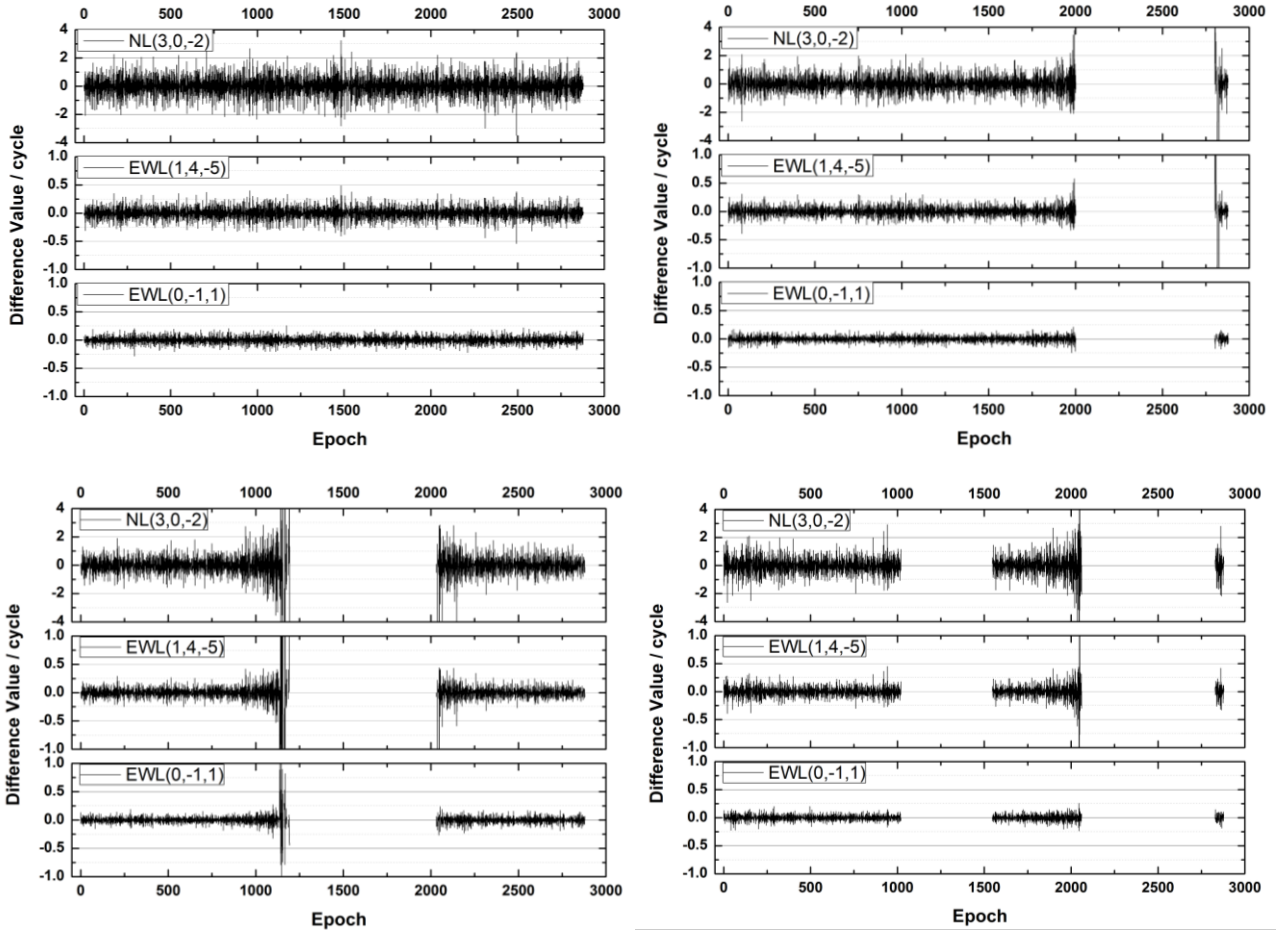

Figure 2. Combination ambiguity difference of satellite C02、C06、C13 and C16 between adjacent epoch for BDS-2 triple frequency

Figure 2 shows the ambiguity difference results of adjacent epochs corresponding to the three-frequency combined ambiguities corresponding to the BDS-2 C02, C06, C13 and C16 satellites from left to right and from top to bottom. Combination ambiguity results for extra-wide lane (0, -1, 1), (1, 4, -5) and narrow lane (3, 0, -2). It can be seen from the figure that the ambiguity difference between adjacent epochs in the extra-wide lane (0, -1, 1) is far less than ±0.5 cycles except for the individual epochs where the C13 satellite is about to be invisible. The method of rounding can be used to fix the single epoch ambiguity. In the extra-wide lane (1, 4, -5), only the C02 satellite is less than ± 0.5 cycles in the whole observation period, and the rest of the satellites have some epoch results exceeding ± 0.5 cycles. In the results of the narrow lane (3, 0, -2), most of the epoch results fluctuate within ±2 cycles, and the individual epochs of C06, C13 and C16 satellites are even larger than ±4 cycles, and it is difficult to use simple direct rounding to fix single epoch ambiguity for whole observation period.

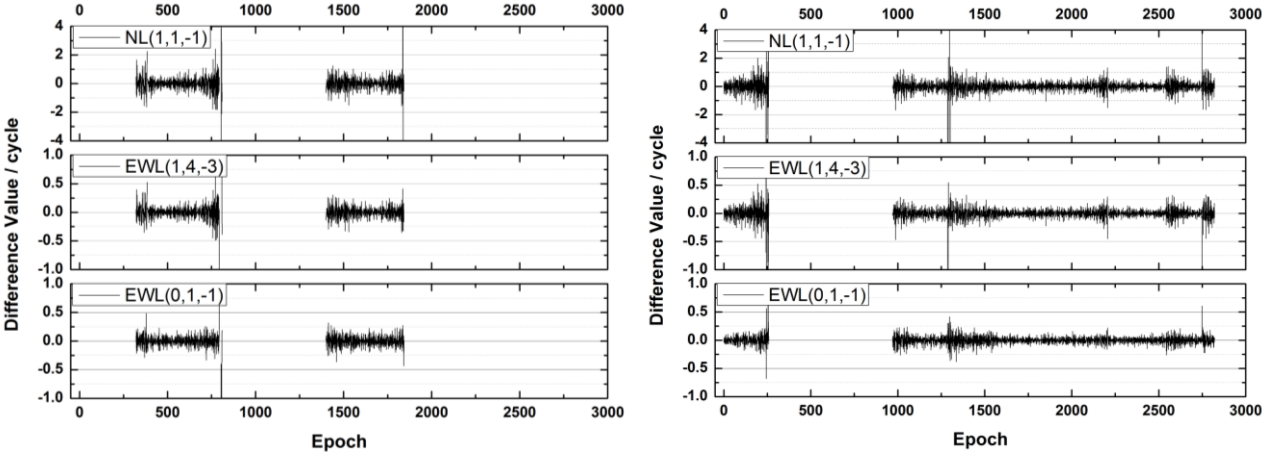

Figure 3. Combination ambiguity difference of satellite C34 and C40 between adjacent epoch for BDS-3 triple frequency

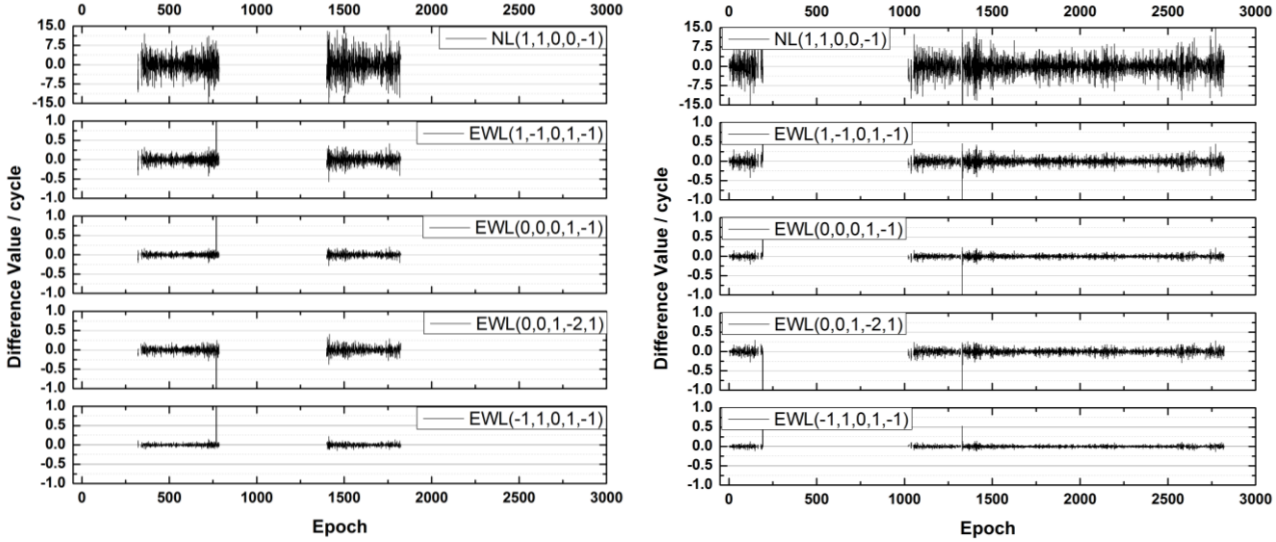

Figure 4. Combination ambiguity difference of satellite C34 and C40 between adjacent epoch for BDS-3 five frequency

Figure 3 shows the difference results of adjacent epochs of three-frequency combined ambiguity corresponding to the BDS-3 C34 and C40 satellites. It can be seen from the figure that the two extra-wide lanes (0, 1, -1) and (1, -4, 3) most of the ambiguity differences between adjacent epochs are less than ±0.5 cycles, and only the results at individual epochs are greater than ±0.5 cycles. However, the ambiguity difference between most adjacent epochs in the combination of narrow lane (1, 1, -1) is less than ±1 cycle, and a small number of epochs exceed ±2 cycles. The results are better than the BDS-2 three-frequency combination ambiguity results.

Figure 4 shows the difference results of the adjacent epochs of the five-frequency combined ambiguity corresponding to the BDS-3 C34 and C40 satellites, respectively. It can be seen from the figure that the difference between the adjacent epochs of the four extra-wide lane combination ambiguities except for individual epochs is less than ±0.5 cycles, and the fluctuation range of narrow-lane combination ambiguity results is much larger than that of BDS-2 and BDS-3 three-frequency combination ambiguity results.

6. CONCLUSION

In this paper, the fuzzy clustering analysis method is used to deal with the selection of multi-frequency GNSS linear combinations such as GPS, BDS-2, BDS-3, Galileo, etc., and the ambiguity of BDS-2 and BDS-3 short baseline combination is solved by GF_MCAR method to verify the validity of the combinations selection results and the following conclusions are obtained.

With the increase in the number of GNSS signals, the number of high-quality combinations has increased sharply. The number of combined signals of five-frequency high-quality extra-wide lanes is about 150 times that of three-frequency, and about 12 times of four-frequency.

The extra-wide lane combination selected by the fuzzy clustering analysis method is suitable for the BDS-2, BDS-3 three-frequency or five-frequency combination ambiguity resolution in the GF_MCAR model, and most of the combination ambiguity differences between adjacent epochs are less than ±0.5 cycles, which can be used for fast resolution of single-epoch ambiguity. However, the result of this model for

narrow-lane combined ambiguity is affected by factors such as the wavelength and noise of the combined observation, as well as the influence of extra-wide lane ambiguity, and it is difficult to directly round and fix in a single epoch. In the future, we will continue to optimize the fast narrow-lane combined ambiguity fixing method of the multi-frequency carrier phase ambiguity resolution.

ACKNOWLEDGMENTS

This work is supported by National Scientific Foundation of China (Nos. 42174003, 41861061 and 42061076), Granted by Gansu Science and Technology Plan (No.21JR7RA318), The Young Scholars Science Foundation of Lanzhou Jiaotong University (No.2020055) and LZJTU EP (No.201806).

REFERENCES

Bai, Z., Zhang, Q., Huang, G. (2019). Real-time BeiDou landslide monitoring technology of "light terminal plus industry cloud". Acta Geodaetica et Cartographica Sinica, 48(11): 1424-1429.

Cheng, Y., Wenzhong, S., & Wu, C. (2018). Correlational inference-based adaptive unscented kalman filter with application in GNSS/IMU-integrated navigation. GPS Solutions, 22(4), 100-.

Cocard, M., Bourgon, S., Kamali, O., & Collins, P. (2008). A systematic investigation of optimal carrier-phase combinations for modernized triple-frequency GPS. Journal of Geodesy, 82(9), 555-564.

Dai, W., Liu, N., Santerre, R. (2016). Dam Deformation Monitoring Data Analysis Using Space-Time Kalman Filter. International Journal of Geo-Information, 5(12):236-250.

Geng, J., Guo, J., Chang, H., & Li, X. (2019). Toward global instantaneous decimeter-level positioning using tightly coupled multi-constellation and multi-frequency GNSS. Journal of Geodesy, 93(7), 977-991.

He, H., Li, J., Yang, Y., Xu, J., Guo, H., & Wang, A. (2014). Performance assessment of single- and dual-frequency BeiDou/GPS single-epoch kinematic positioning. GPS Solutions, 18(3), 393-403.

Huang, L., Song, L., Liu, X. (2011). Optimalzation and Selecetion of GPS Triple-carriers Phase Combination Observations Based Self-adaptive Clustering Algorithm. Journal of Geodesy and Geodynamics, 31(4):99-102.

Li, J., Yang, Y., Xu, J., He, H., & Guo, H. (2015). GNSS multi-carrier fast partial ambiguity resolution strategy tested with real BDS/GPS dual- and triple-frequency observations. GPS Solutions, 19(1), 5-13.

Li, B. (2018). Review of triple-frequency GNSS: ambiguity resolution, benefits and challenges. Journal of Global Positioning Systems, 16(1), 1.

Li, J., Yang, Y., Xu, J., He, H. (2012). Optimal Carrier-phase Combinations for Triple-frequency GNSS Derived from an Analytical Method. Acta Geodaetica et Cartographica Sinica, 41(6):797-803.

Li, J., Yang, Y., He, H., & Guo, H. (2017). An analytical study on the carrier-phase linear combinations for triple-frequency GNSS. Journal of Geodesy, 91(2), 151-166.

Li, Y., Yan, H., Wang, S., Yang, W. (2020). Fuzzy Cluster Analysis Method to Select Optimal Combinations for Triple-frequency BDS[J]. Acta Geodaetica et Cartographica Sinica, 49(8): 974-982.

Li, Y., Yan, H., Yang, W., Wang, S. (2021). Ambiguity Resolution of BDS Long Baseline Based on Fuzzy Clustering Analysis Method[J]. Journal of Geodesy and Geodynamics, 41(10): 1040-1044.

Teunissen, P., Odolinski, R., & Odijk, D. (2014). Instantaneous Beidou + GPS RTK positioning with high cut-off elevation angles. Journal of Geodesy, 88(4), 335-350.

Wen, W., Zhang, G., & Li mil a Hsu. (2019). Correcting NLOS by 3d lidar and building height to improve GNSS single point positioning. Navigation, 66(4), 705-718.

Yang, Y. X., Li, J. L., Xu, J. Y., Tang, J., & He, H. B. (2011). Contribution of the compass satellite navigation system to global PNT users. Chinese Science Bulletin, 56(26), 7.

Yang, Y., Li, J., Xu, J., & Tang, J. (2011). Generalised dops with consideration of the influence function of signal-in-space errors. Journal of Navigation, 64(S1), S3-S18.

Yang, C., Shi, W., Chen, W. (2016). Comparison of Unscented and Extended Kalman Filters with Application in Vehicle Navigation. Journal of Navigation, 70(2):1-21.

Zhonghai, Y., Cuilin, K., Yarong, W., Wenkun,Y., Changsheng, C., Wujiao, D. (2018). Combination of high- and low-rate GPS receivers for monitoring wind-induced response of tall buildings. Sensors, 18(12):4100.

Zhang, Z. , Li, B. , He, X. , Zhang, Z. , & Miao, W. . (2020a). Models, methods and assessment of four-frequency carrier ambiguity resolution for beidou-3 observations. GPS Solutions, 24(4).

Zhang, Z., Li, B., He, X. (2020b). Geometry-free single-epoch resolution of BDS-3 multi-frequency carrier ambiguities. Acta Geodaetica et Cartographica Sinica, 49(9): 1139-1148.

Zhang, Q., Huang, G., Yang, C. (2017). Precision Space Observation Technique for Geological Hazard Monitoring and Early Warning. Acta Geodaetica et Cartographica Sinica, 46(10): 1300-1307.

Zhang, X. H., He, X. (2015). Bds triple-frequency carrier-phase linear combination models and their characteristics. Science China: Earth Sciences, 45(5):601-610.

Zhang, X., Zhang, Y., Li, B., Qiu, G. (2018). GNSS-based verticality monitoring of super-tall buildings. Applied Sciences, 8(6), 991-1005.

Zhu, H., Li, J., Xu, A. (2020). High-Precision BDS Augmented Positioning Method for Disaster Emergency Environment on Smart Device. Geomatics and Information Science of Wuhan University, 45(8): 1155-1167.